Surface band structures on Nb(001)

B.-S. Fang
User's Division, Synchrotron Radiation Research Center, Hsinchu, Taiwan 300, Republic of China and Department of Physics, National Tsing-Hua University, Hsinchu, Taiwan 300, Republic of China

W.-S. Lo
Department of Physics, National Tsing-Hua University, Hsinchu, Taiwan 300, Republic of China

T.-S. Chien
User's Division, Synchrotron Radiation Research Center, Hsinchu, Taiwan 300, Republic of China

T. C. Leung and C. Y. Lue
Department of Physics, National Chung-Cheng University, Chia-Yi, Taiwan 621, Republic of China

C. T. Chan and K. M. Ho
Ames Laboratory, Department of Physics, Iowa State University, Ames, Iowa 50011
(Received 30 November 1993; revised manuscript received 26 April 1994)

We report the joint studies of experimental and theoretical surface band structures of Nb(001). Angle-resolved photoelectron spectroscopy was used to determine surface-state dispersions along three high-symmetry axes $\bar{\Gamma}\bar{M}$, $\bar{\Gamma}\bar{X}$, and $\bar{M}\bar{X}$ in the surface Brillouin zone. Ten surface bands have been identified. The experimental data are compared to self-consistent pseudopotential calculations for the 11-layer Nb(001) slabs that are either bulk terminated or fully relaxed (with a 12% contraction for the first interlayer spacing). The band calculations for a 12% surface-contracted slab are in better agreement with the experimental results than those for a bulk-terminated slab, except for a surface resonance near the Fermi level, which is related to the spin-orbit interaction. The charge profiles for all surface states or resonances have been calculated. Surface contraction effects on the charge-density distribution and the energy position of surface states and resonances will also be discussed.

I. INTRODUCTION

The nonrelativistic bulk energy-band dispersions of most of the bcc transition metals, such as tantalum, niobium, tungsten, and molybdenum are quite similar.[1–4] Only the relative energy position of the Fermi level (E_F) to the triply degenerate d states at $\Gamma_{25'}$ varies. The variation, however, is very important in understanding both electronic and structural properties of such metal surfaces. Relativistic effects, mainly the spin-orbit interaction, induce energy splitting of this triply degenerate state. The energy splitting is accompanied with symmetry hybridization and band noncrossing. A pseudo-energy-gap is therefore created. The surface electronic structure has been found to be affected in two ways: (1) New surface resonances might be created[5–7] inside the gap or an existing surface resonance may be moved to the gap.[8] (2) The existence of the relativistic gap modifies dispersion relations of the surface energy bands nearby.[9,10] Such effects only appear within a limited energy region in the vicinity of the relativistic gaps. For the metals with $\Gamma_{25'}$ below E_F, such as tungsten and molybdenum, the spin-orbit effect must be considered in order to understand the photoemission results of the surface electronic structure. For Ta(001),[11] where $\Gamma_{25'}$ is about 1 eV above E_F, no trace of the spin-orbit effect was found in the experimental results of surface resonances. Instead, the surface-layer relaxation plays a major role in understanding the surface bands.

The interplay between electron charges and surface-layer relaxations is rather complicated. The first model to explain the inward relaxation of a surface layer is the Smoluchowski effect.[12,13] Electronic charge density becomes smoother to reduce surface corrugation upon its creation. This smoothing process is equivalent to redistributing charge from the region right above the surface atoms to the hollows between them. It adds more charge to the surface layer and gives rise to a net inward electrostatic force on the top-layer nuclei. The inward relaxation is more pronounced for rougher surface such as the (001) plane of bcc metals. Another model, which focuses on transition metals, indicates that the d electrons provide an additional inward-relaxation contribution to the surface layer[14,15] as a result of spill out of the sp electrons to the vacuum and the unchanged d bonds between the first two layers. However, the importance of the surface-layer relaxation in surface band calculations depends on the magnitude of relaxation of the first interlayer spacing relative to the bulk-terminated lattice. In the case of a small surface relaxation, a 6% contraction relative to the bulk interlayer spacing of W(001) (Ref. 16), for example, the theoretical study on surface electronic structures, lo-

cal density of states, work function, and core-level shifts cannot find a significant difference between contracted and uncontracted surfaces. For the 14% contraction of the Ta(001) surface,[11] the energy position of some surface resonances shifts to the higher binding-energy side due to the increasing charge density localized in between the first two layers. The contraction also induces a new surface resonance with odd symmetry.

The Δ_1 bulk band along the high-symmetry direction ΓH (i.e., the [001] direction) has been determined by an angle-resolved photoemission study.[17] No bulk state appeared in the energy region between -2.3 eV and E_F. It confirmed the prediction of many nonrelativistic calculations with different methods.[3,4,18–20] However, with the higher energy resolution,[8] a bulk state to -0.2 eV was separated from the surface state reported in Ref. 17. Followed by a relativistic calculation with a tight-binding method, it was suggested that the spin-orbit effect was responsible for the appearance of the bulk state below E_F. Similar to other studies, the spin-orbit interaction splits off the triply degenerate d states at $\Gamma_{25'}$, which are just above E_F for Nb, and creates a pseudo energy gap. The energy splitting is about 0.25 eV and is large enough to expel part of the bulk band down below E_F. The spin-orbit interaction also significantly shifts the energy position and modifies the dispersion relation of surface bands near E_F. The spin-orbit interaction effect vanishes away from the vicinity of the pseudo energy gap. The experimental finding of a surface resonance at -0.6 eV agreed with the theoretical results of a nonrelativistic calculation with a nonlocal self-consistent pseudopotential scheme.[21]

In this paper, we report angle-resolved photoemission studies of the two-dimensional band structure for the (001) surface of niobium. It is not surprising that the experimental results show some discrepancies to the earlier nonrelativistic calculations assuming an ideal surface.[21] The behavior of the surface bands near E_F can be explained by introducing the spin-orbit effect. However, there are some other aspects of the measured surface band structures that are similar to the earlier theoretical calculation. Our own photoelectron-diffraction study[22] of Nb(001) indicates a substantial [$(13\pm5)\%$] contraction of the first interlayer spacing. Some of the discrepancies between the current measurement and the theoretical calculation may be resolved if surface relaxations are taken into account. At least in the case of Ta(001), it is known that such a degree of relaxation (14%) does modify the surface electronic structure. We thus performed a surface band calculation within the local-density-functional formalism and with interlayer spacings determined by fully relaxing the system with force calculations. We obtained a 12% relaxation for the outermost interlayer spacing, in good agreement with our own experimental results, and the surface band structure also agrees better with the experiment when the surface is fully relaxed. The surface contraction and spin-orbit interaction are found to play an important role in understanding electronic properties of the Nb(001) surface.

The remainder of this paper is organized as follows: The experimental procedure will be presented in Sec. II. The theoretical calculations will be described briefly in Sec. III. In Sec. IV, the angle-resolved photoemission results of surface energy bands will be presented and discussed together with the theoretical results calculated from a 12% contracted surface. The charge-density variation due to the surface contraction will be also described. Finally, the conclusion will be made in Sec. V.

II. EXPERIMENTAL PROCEDURE

A single-crystal Nb(001) of 99.999% purity, about 0.5 in. in diameter, was mechanically polished and chemically cleaned before being attached to tungsten rods. The rods were mounted to a sample holder that sits on a rotary table and a manipulator with x-y-z linear motion. Temperature variation of the sample, in the range between 150 to 2500 K, could be reached by liquid-nitrogen cooling and electron-bombardment heating. The surface was cleaned with a conventional method[17] and characterized with Auger spectroscopy, low-energy electron diffraction, and valence-band photoelectron spectroscopy. The experiment was carried out in an angle-resolved photoemission chamber of the in-house Photoemission Laboratory at Synchrotron Radiation Research Center (SRRC). The energy resolution of the analyzer was always set at 0.1 eV, and was occasionally tuned to 25 meV in order to determine the near Fermi-level structures. He(I), He(II), and Ne(I) were used to excite photoelectrons from the Nb(001) surface. The experimental setup was arranged to allow the high-symmetry line $\bar{\Gamma}\bar{X}$ (or $\bar{\Gamma}\bar{M}$) lying on the rotation plane of the analyzer. A two-angle method was used to map out the surface band structures along other high-symmetry lines, i.e., $\bar{\Gamma}\bar{M}$ (or $\bar{\Gamma}\bar{X}$) and $\bar{X}\bar{M}$. Results from the two-angle method have been compared to those measured from a polar angle scan along the same symmetry line. The agreement was quite good. The base pressure of the chamber was 6×10^{-11} Torr. It rose up to 2×10^{-10} Torr when spectra were taken. As a precaution, the sample was annealed up to 2000 K every 20 min.

III. THEORETICAL METHOD

In this section, we will discuss briefly the computational process. The calculation presented here are performed within the local-density-functional formalism,[23] with the Hedin-Lundqvist form of local exchange-correlation potential. Norm-conserving pseudopotentials are used to describe the core-valence interaction. The quality of the angular-momentum-dependent pseudopotentials has been examined by comparing with all-electron eigenvalues and excitation energies for various atomic configurations; details have been published previously.[23] A mixed-basis set comprised of both plane waves and local orbitals is used to expand the Bloch functions. The mixed-basis pseudopotential approach has been successfully used to study various transition-metal systems.[19,24] In particular, structural properties of bulk Nb are in very good agreement with experimental values.[23] A slab of Nb orientated in the (001) direction is used to simulate the (001) surface, and slabs up to 11 layers thick are used in the present calculations. A supercell geometry (i.e., repeated slabs separated by vacuum) is used, and the vacuum thickness

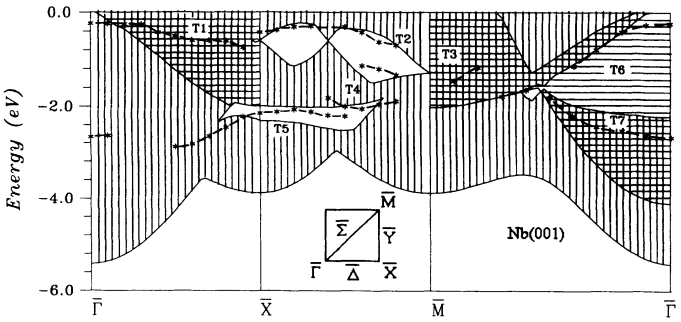

FIG. 1. The projected band structures are displayed with vertical and horizontal solid lines. The surface states (or surface resonances), as determined by an ideal 11-layer slab for the Nb(001) surface, are marked with "*," connected by dashed lines for visual convenience. The inset at the bottom is a surface Brillouin zone of the (001) face.

is about 12.3 a.u. All the results presented are fully self-consistent, and the charge, the electron screening potential, and the electronic eigenvalues are sampled with a uniform grid of 21 k points in the irreducible surface Brillouin zone (SBZ). The Fourier components of the screening potential are self-consistent to within 10^{-6} Ry. All the interlayer distances are fully relaxed by computing the Hellmann-Feynman forces,[25] until the maximum force acting on the atoms are smaller than 0.02 Ry/a.u. We find a 12% inward relaxation for the outermost layer. Relaxations for innerlayers are small.

The surface states and surface resonances are determined with the help of the following criteria. First, bona-fide surface states should exist inside energy gaps in the projected bulk band structure (PBS) onto the (001) surface. In high-symmetry directions, the surface states transforming according to some specific irreducible representations can also exist in "symmetry gaps" of the PBS. Therefore, the first step involves the projection of the bulk band structure onto the SBZ of the (001) surface. Then we look for eigenstates in the slab calculations that falls inside the energy gaps of the projected band. The energy bands along $\bar{\Gamma}$-$\bar{X}$-$\bar{M}$-$\bar{\Gamma}$ in the SBZ for Nb(001) are shown in Fig. 1 (ideal 11-layer slab) and Fig. 2 (relaxed 11-layer slab), respectively. The inset at the bottom of Fig. 1 is a diagram of the (001) SBZ. Also shown in these figures are some of the symmetry gaps along the symmetry lines. Symmetry gaps are gaps at high-symmetry points or along symmetry lines in the PBS in which bulk states of a given symmetry are forbidden, but where states of other symmetry may exist. In these figures, vertical crosshatching denotes the extent of bulk states with Δ_1, $Y_{1,2}$, and Σ_1 symmetry, while horizontal crosshatching is used to show the extent of bulk states with Δ_2 and Σ_2 symmetry (see Ref. 21). The surface relaxation improves the agreement between theoretical and experimental results as shown in the following sections. Along the $\bar{\Gamma}$-$\bar{M}$ direction, noticeable changes accompany the surface contraction. We identified five surface bands for the relaxed slab, while the unrelaxed slab has only three surface bands. Also, the surface band $T6$ shifts downward by about 0.2 eV when the surface is relaxed. Along the $\bar{\Gamma}$-$\bar{X}$ direction, there are almost no influences on the surface states, except that we have an extra surface band $T8$ in the relaxed slab calculation.

We also calculate the charge profile along the (001) direction (i.e., the "z" direction). The charge profile is defined as

$$\rho(z)=\int\int dx\,dy\,\rho(\mathbf{r})\ .$$

Surface states and strong resonances are, by definition, those that are localized on the surface layers and decay rapidly into a bulk. For states that are not residing in forbidden gaps, we label them as surface resonances if the charge is strongly localized on the top surface layers. The criteria for "strongly localized" is necessarily subjective for thin slab calculations. Nevertheless, the inspection of $\rho(z)$ gives us a very useful and intuitive way of finding surface states and resonances. In the present calculation, we search for states that have 60% or more of their charge localized on the top two layers of the slab. The charge profile for some of the surface states and resonances will be discussed in Sec. IV D.

IV. RESULTS AND DISCUSSION

All surface states identified in this work have been characterized with three different photon energies 16.8, 21.2, and 40.8 eV. A typical example is shown in Fig. 3. By selecting appropriate emission angles to 13.1°, 41.7°,

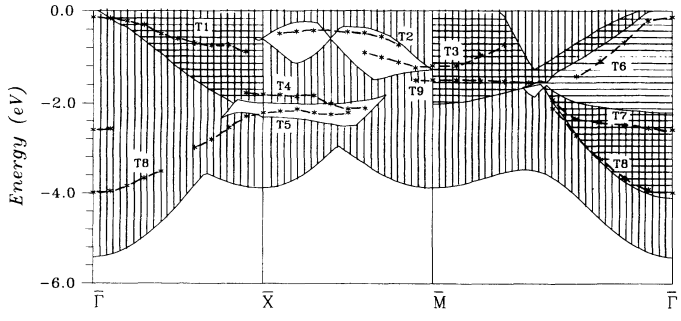

FIG. 2. The projected band structures are displayed with vertical and horizontal solid lines. The surface states (or surface resonances), as determined by a fully relaxed 11-layer slab for the Nb(001) surface, are marked with "*," connected by dashed lines for visual convenience.

and 51.7° referred to the surface normal along the $\bar{\Gamma}\bar{M}$ symmetry line, two surface features $S9$ and $S3$ at $\bar{M}$ appears in three energy distribution curves [EDC's, solid lines] measured with photon energies of 40.8, 21.2, and 16.8 eV, respectively. The $S9$ peak is predominant in the spectra while $S3$ emission is vaguely seen, and their binding energies are -1.3 and -1.0 eV with respect to E_F, respectively. Their energy positions are invariant with different photon energies, indicating that they are good candidates for two-dimensional states. The feature lying on the higher binding-energy side of $S9$, marked as B, shows dispersion with varying photon energies, and thus has the character of a three-dimensional state. Another test to distinguish the surface feature from the bulk is to add impurity onto the surface. The surface feature is expected to be sensitive to impurity adsorption. In Fig. 3, the dotted line corresponds to the EDC for $h\nu=21.2$ eV, which was measured after the Nb(001) surface was dosed with 5-L H_2. Clearly, the surface feature shows a dramatic change both in the energy position and peak intensity. On the contrary, the bulk peak remains unaffected. All the surface bands selected in this paper appear at stationary energy position (± 0.1 eV) at fixed $K_\parallel$ via the change of photon energies. The impurity test was performed only at symmetry points.

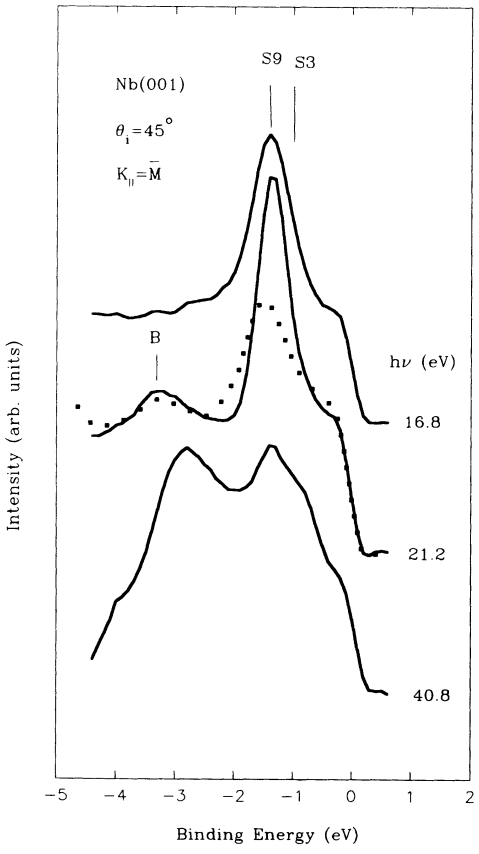

FIG. 3. Angle-resolved photoelectron spectra for the surface states at $\bar{M}$ measured with three different photon energies (16.8, 21.2, and 40.8 eV). The solid line "——" is for a clean surface and the dotted line "· · ·" is for a 5-L H_2 covered surface. The angle of incidence is 45°.

A. Surface band dispersions along $\bar{\Gamma}$-$\bar{M}$

Figure 4 shows $h\nu=21.2$ eV EDC's at different $K_\parallel$ along $\bar{\Gamma}$-$\bar{M}$. The surface states are selected from the band mapping results with different photon energies. Six surface bands marked as $S0$, $S3$, $S6$, $S7$, $S8$, and $S9$ are observed. In the region between 0.56 $\bar{\Gamma}\bar{M}$ and 0.71 $\bar{\Gamma}\bar{M}$, the spectra are quite complex, and the band connectivity is somewhat arbitrary.

Both the $S0$ and $S6$ bands start from $\bar{\Gamma}$ at a binding energy of -0.060 eV. They disperse downward and their intensities increase with increasing $K_\parallel$ until the split off occurs around $K_\parallel=0.11$ $\bar{\Gamma}\bar{M}$. It is hard to judge whether $S0$ crosses E_f or not. The $S7$ band gradually hybridizes with bulk states along $\bar{\Gamma}$-$\bar{M}$, and shows large dispersion beyond 0.47 $\bar{\Gamma}\bar{M}$. The separation of $S3$ and $S0$ and of $S6$ and $S9$ is somewhat arbitrary, mainly referred to abrupt changes in binding energies and to the symmetry of projected bulk bands where these surface features can be located. Along Γ-$\bar{M}$, as shown in Fig. 4, the intensity of the $S9$ peak gradually increases while $S3$ decreases. Then at M, the former is predominant while $S3$ is nearly invisible. The $S8$ band is very short, appearing only in the vicinity of $\bar{\Gamma}$.

Figure 5 shows the PBS and the surface bands (thick solid curves) from the self-consistent calculations for the relaxed 11-layer niobium slab along $\bar{\Gamma}$-$\bar{M}$. The experimental surface bands and resonances are plotted as dot

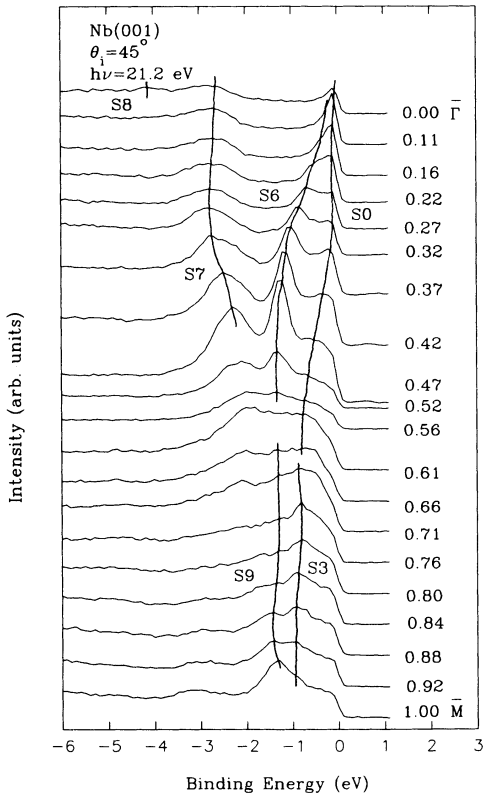

FIG. 4. Angle-resolved photoelectron spectra for the surface states (resonances) taken at various polar angles along $\bar{\Gamma}$-$\bar{M}$. The photon energy is 21.2 eV and the angle of incidence is 45°.

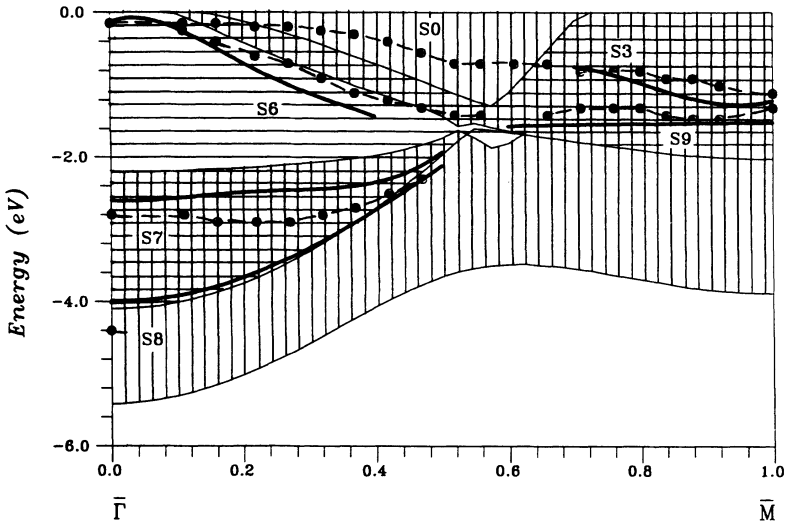

FIG. 5. Dispersion of the surface states (resonances) on Nb(001) along $\bar{\Gamma}$-$\bar{M}$. Dash and dots are experiment results, the shaded area represents the projected bulk bands, and the sold lines are calculated surface states or resonance from the relaxed Nb(001) slab.

and dashes. From Fig. 5, we can see that the $S0$ band near $\bar{\Gamma}$ lies in the even-symmetry gap. The $S6$ band disperses down to higher binding energy along the edge of an even-symmetry gap. The $S3$ surface resonance starts from -0.8 eV at $K_{\parallel}=0.64$ $\bar{\Gamma}\bar{M}$ and disperses to -1.0 eV at $\bar{M}$. The surface resonance $S9$ starts from -1.1 eV at about $K_{\parallel}=0.6$ $\bar{\Gamma}\bar{M}$ and passes $\bar{M}$ with a binding energy of -1.3 eV. Both $S3$ and $S9$ are surface resonances consisting mainly of the $d_{(x2-y2)}$ and $d_{(x-y)z}$ orbitals. The $S8$ band is much shorter compared with the theoretical result. The $S9$, $S8$, and part of the $S3$ bands can only be identified in the band calculation that has a 12% surface contraction, but not in the calculation with an ideal surface. We will go back to this point later. The $S7$ band, with even symmetry, is a surface resonance and becomes more bulklike at $K_{\parallel}>0.47$ $\bar{\Gamma}\bar{M}$.

Figure 6 displays the normal emission ($K_{\parallel}=0$) EDC's for a clean surface (the solid line) and a 0.1-L O_2 covered surface (the dotted line) of Nb(001). As can be seen from Fig. 6, the $S8$ state is very sensitive to surface contaminants, i.e., its peak intensity is quenched and peak position is shifted. It was assigned as a Δ_1 bulk state by Fang, Ballentine, and Erskine[17] since it has a little dispersion with photon energies. However, in this work it was instead assigned as a surface resonance that highly hybridizes with the Δ_1 bulk states. Nevertheless, it is too broad to pin accurately down its peak position. From the theoretical calculation, the profile of the charge density indicates that the $T8$ and at $\bar{\Gamma}$ has only about 60% of the wave function at the surface region, that is, it is highly hybridized with the Δ_1 bulk states. In contrast, the $T1$ state at $\bar{\Gamma}$ is a bona-fide surface state, which resides in an s-d hybridized gap, and it has about 99% of the wave function at the surface region. Furthermore, it has been reported that the surface resonances, which highly hybridizes with bulk states, could disperse significantly up to ~ 1.0 eV.[26] Therefore, we conclude that $T8$ at $\bar{\Gamma}$ is a surface resonance, although it appears to have some dispersion with the variation of photon energies.

It is worth mentioning that the $S0$ band is neither predicted from the ideal surface calculation nor from the relaxed surface. It is quite plausible that this band is due to the spin-orbit-interaction effects, since its binding energy is in the vicinity of the relativistic pseudo energy gap.[8] The projection of the relativistic bulk bands onto the (001) plane surface and more photoemission studies with polarized photon beams are needed to make a decisive conclusion on the relation between the existence of $S0$ and the spin-orbit interaction effects.

B. Surface band dispersions along $\bar{X}$-$\bar{M}$

Figure 7 shows the selected EDC's measured with $h\nu=21.2$ eV at different $K_{\parallel}$ along the $\bar{X}$-$\bar{M}$ axis. The

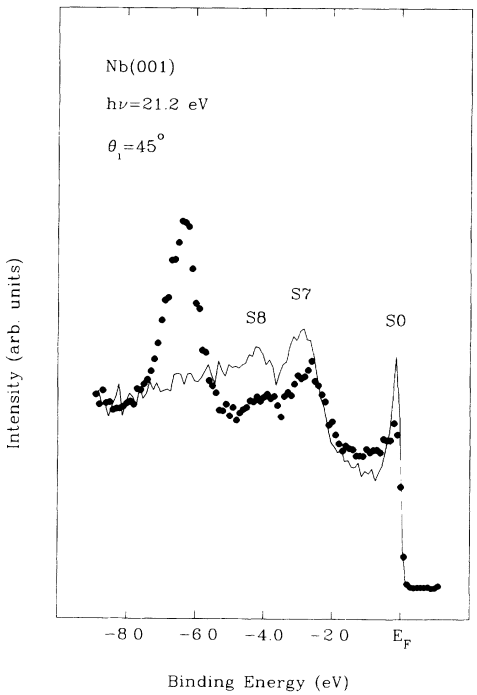

FIG. 6. Normal-emission ($K_{\parallel}=0$) electron energy distribution curves for a clean (solid line) surface and a 0.1-L O_2 covered (dotted line) surface of Nb(001) at $h\nu=21.2$ eV.

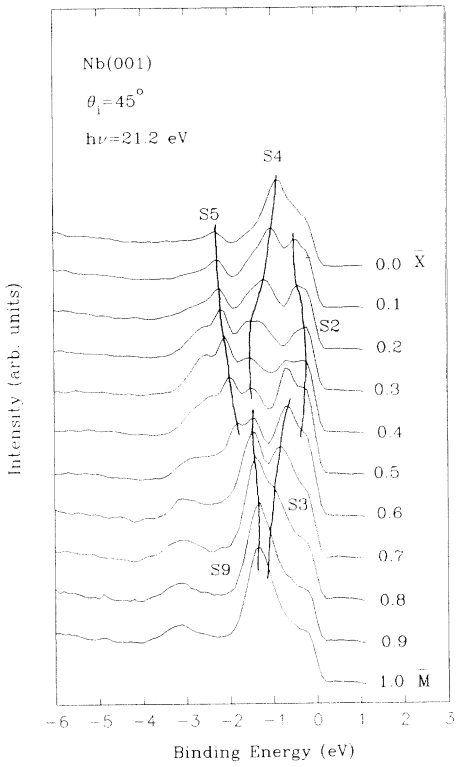

FIG. 7. Angle-resolved photoelectron spectra for the surface states (resonances) taken at various $K_{\parallel}$ along $\bar{X}$-$\bar{M}$. The photon energy is 21.2 eV and the angle of incidence is 45°.

corresponding band calculation is shown in Fig. 8. There are five surface bands marked as $S2$, $S3$, $S4$, $S5$, and $S9$. The $S2$ band starts from -0.5 eV at about 0.1 $\bar{X}\bar{M}$. It disperses to lower binding energies until $K_{\parallel}=0.3$ $\bar{X}\bar{M}$, after which the dispersion turns back and goes to -0.5 eV at 0.6 $\bar{X}\bar{M}$. The $S3$ band in the region of $K_{\parallel}<0.6$ $\bar{\Gamma}\bar{M}$ is prone to bulk characteristics. It starts from -0.6 eV at 0.6 $\bar{X}\bar{M}$ and moves to -1.0 eV at $\bar{M}$. Its intensity decreases gradually along $\bar{X}$-$\bar{M}$, and becomes almost invisible at $\bar{M}$. Similar intensity attenuation is also found for this band along $\bar{\Gamma}$-$\bar{M}$. The $S4$ band disperses downwards from -0.8 eV at $\bar{X}$ to -1.5 eV at 0.5 $\bar{X}\bar{M}$. The $S5$ band disperses upwards from -2.3 eV at $\bar{X}$ to -1.8 eV at 0.6 $\bar{X}\bar{M}$. The $S9$ band starts from -1.4 eV near 0.6 $\bar{X}\bar{M}$, the passes $\bar{M}$ and extends into the SBZ along $\bar{\Gamma}$-$\bar{M}$. The connectivity between $S4$ and $S9$ is somewhat arbitrary, and the choice here is according to the theoretical band structure.

As shown in Fig. 8, the $S2$, $S3$, and $S5$ bands reside mainly in the absolute gaps. Note that the $S2$ band agrees with the theoretical $T2$ band quite well. The $S5$ band is inside an absolute gap near -2.0 eV, and has a subsurface-state character, as will be described later. The energy of the $S4$ band lies above the calculated band $T4$ by about 0.8 eV. The $S9$ band exists along the edge of an absolute gap. The distinction of $S9$ and $S4$ is mainly deduced from the band calculation.

Figure 9 displays the photoemission spectra for the surface states at $K_{\parallel}=0.4$ $\bar{X}\bar{M}$ measured with 16.8-, 21.2-, and 40.8-eV photon energies. The emission angles were selected so as to keep $K_{\parallel}$ fixed at 0.4 $\bar{X}\bar{M}$ for different photon energies. From this figure, we obtain two important information: (1) $S3$ loses its surface characteristics for $K_{\parallel}<0.5$ $\bar{\Gamma}\bar{M}$, and (2) $S5$ is mainly a subsurface band. The energy positions of the $S2$, $S5$, and $S4$ bands remain unchanged, showing a characteristic of a two-dimensional state. However, the photoemission peak marked as B at -0.6 eV in the $h\nu=21.22$ eV EDC, which is on the energy dispersion track of $S3$, either disappears or shifts to different energies with varying $h\nu$, a characteristic of a three-dimensional state. To distinguish a subsurface state from a surface state, Fang, Ballentine, and Erskine[17] have found an enhancement of photoelectron cross section of subsurface state around the bulk plasma frequency ω_p ($\approx$20.0 eV for Nb), but a decreasing intensity at the surface plasma frequency ω_s ($\approx$14.0 eV for Nb). However, the magnitude of the photoelectron cross section of surface states varies oppositely. In Fig. 9, the $S5$ state has an intensity enhancement at $h\nu=21.2$ eV, which is close to ω_p, and an intensity decreasing at $h\nu=16.8$ eV, which is close to ω_s. Such vari-

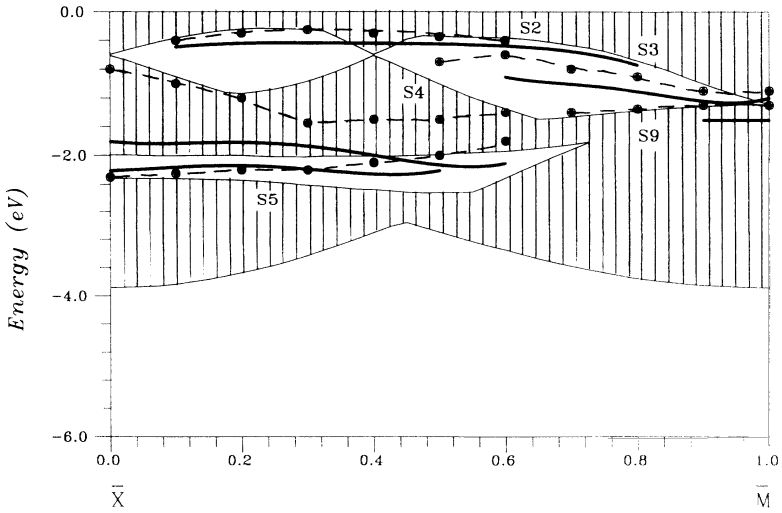

FIG. 8. Dispersion of the surface states (resonances) on Nb(001) along $\bar{X}$-$\bar{M}$. Dash and dots are experiment results, the shaded area represents the projected bulk bands, and the solid lines are calculated surface states or resonances for the relaxed Nb(001) slab.

ation suggests that $S5$ behaves like a subsurface state. The charge-density calculation agrees well with this experimental observation and will be discussed in the later section.

C. Surface band dispersions along $\bar{\Gamma}$-$\bar{X}$

Figure 10 shows selected EDC's measured with $h\nu=21.2$ eV at different $K_\parallel$ along the $\bar{\Gamma}$-$\bar{X}$ axis. The corresponding band calculation is shown in Fig. 11. There are six surface bands marked as $S0$, $S1$, $S4$, $S5$, $S7$, and $S8$. It has been suggested[11] that the $S0$ and $S1$ bands in the vicinity of the relativistic gap would be modified by the spin-orbit interaction effects. The $S0$ band starts from -0.060 eV at $\bar{\Gamma}$, and splits off the $S1$ band around $K_\parallel=0.16$ $\bar{\Gamma}\bar{X}$, then moves upwards and crosses E_F near 0.38 $\bar{\Gamma}\bar{X}$. The $S1$ band can be observed nearly along the entire $\bar{\Gamma}$-$\bar{X}$ direction. It splits off from the $S0$ band, then disperses downwards to -0.60 eV at 0.5 $\bar{\Gamma}\bar{X}$ and ends at -0.40 eV at 0.9 $\bar{\Gamma}\bar{X}$. The $S4$ band initiates from -1.1 eV at about 0.8 $\bar{\Gamma}\bar{X}$ and disperses to -0.8 eV at $\bar{X}$. The $S5$ band emerges from $\bar{X}$ with a binding energy of -2.3 eV and disappears at around 0.64 $\bar{\Gamma}\bar{X}$.

As can be seen from Fig. 11, the $S0$, $S1$, and $S4$ bands are surface resonances. The $S5$ band disperses along the edge of an absolute gap, and moves inside the gap near $\bar{X}$. The $S1$ and $S5$ bands agree quite well with the calculated results. The $S7$ and $S8$ band are much shorter compared to the theoretical results, and their intensities quickly diminish off $\bar{\Gamma}$. The $S7$ band at $\bar{\Gamma}$ has been assigned as a subsurface resonance by Fang, Ballentine, and Erskine.[17] The $S8$ band may also be a surface resonance, although it disperses a little with photon energies.

D. Charge density of surface state and resonances

The $T1$ (corresponding to the $S1$) band lies just below E_F, and the charge of this band is mainly located on and above the top atomic layer. These states are of even symmetry with respect to the $\bar{\Gamma}$-$\bar{X}$ reflection plane. Along $\bar{\Gamma}$-$\bar{X}$, we observe a gradual shift of the charge distribution from the vacuum region to the first atomic layer. The interacted charge on the top two layers decreases rapidly towards the $\bar{X}$ point, so that this band becomes a weak resonance near $\bar{X}$. The surface band $T2$ ($S2$), along the $\bar{X}$-$\bar{M}$ direction, lies inside an absolute gap. The charge of these surface states resides near the first atomic layer as well as between the first and the second atomic layers. The charge profiles for the $T3$ ($S3$) surface states peak in the interlayer region between the first and the second atomic layers along the $\bar{\Gamma}$-$\bar{M}$ direction. They also show some accumulation on the first layer. For the surface states in the $T5$ ($S5$) band, which lies in an absolute gap about 2 eV below E_F, the charge is mainly distributed near the top layer at $\bar{X}$ and along $\bar{\Gamma}$-$\bar{X}$, while along $\bar{X}$-$\bar{M}$ the charge is concentrated near the second layer. These

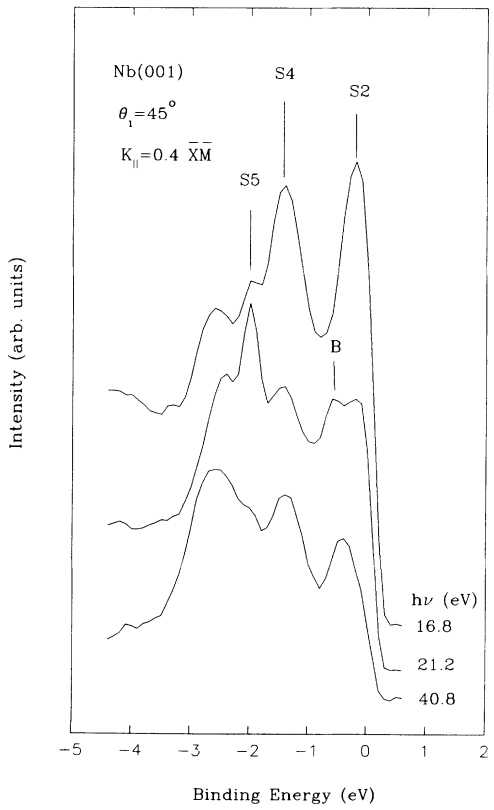

FIG. 9. Angle-resolved photoelectron spectra for the surface states at $K_\parallel=0.4$ $\bar{X}\bar{M}$ measured with three different photon energies (16.8, 21.2, and 40.8 eV). The angle of incidence is 45°.

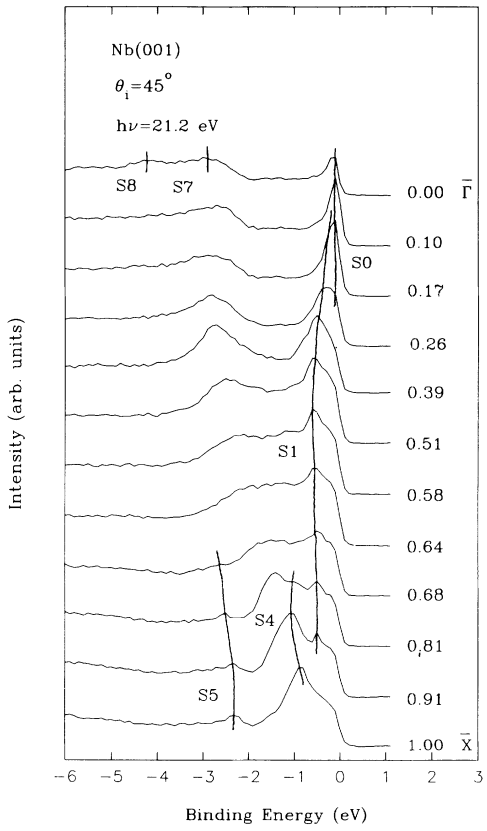

FIG. 10. Angle-resolved photoelectron spectra for the surface states (resonances) taken at various polar angles along $\bar{\Gamma}$-$\bar{X}$. The photon energy is 21.2 eV and the angle of incidence is 45°.

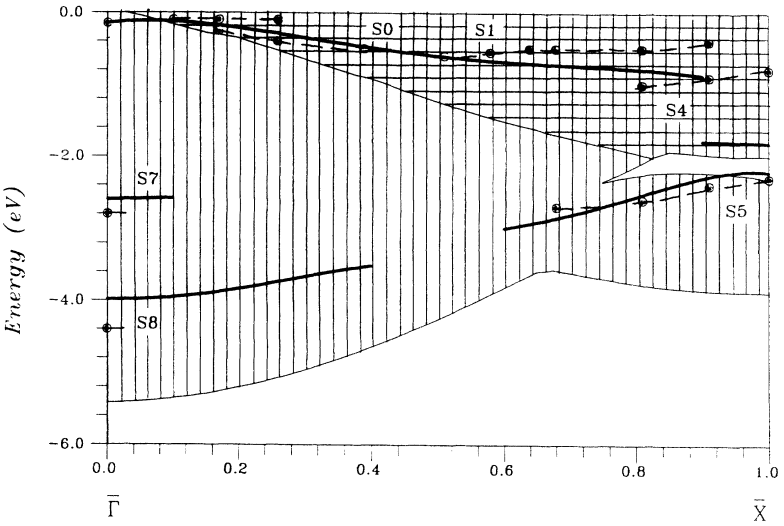

FIG. 11. Dispersion of the surface states (resonances) on Nb(001) along $\bar{\Gamma}$-$\bar{X}$. Dash and dots are experimental results, the shaded area represents the projected bulk bands, and the solid lines are calculated surface states or resonances for the relaxed Nb(001) slab.

surface states ($T5$) are of even symmetry with respect to the $\bar{\Gamma}$-$\bar{X}$ reflection plane. $T6$ ($S6$) is a rather dispersive surface band. From $\bar{\Gamma}$ to $\bar{M}$, there is a noticeable shift of the charge distribution from the first to the second atomic layer. The charge profiles for the $T9$ ($S9$) band are highly localized in between the first and the second atomic layers with a very weak tail extending to the bulk.

Figure 12 presents selected charge profiles for surface states or resonances, which are calculated from the relaxed (12% top-layer contraction) 11-layer slab at different $K_{\parallel}$. The $\bar{\Gamma}$ point is denoted as (0.00, 0.00), $\bar{X}$ as (1.00, 0.00), and $\bar{M}$ as (1.00, 1.00) in this figure. Figure 12(a) shows the charge density of the surface state near E_F at $\bar{\Gamma}$. About 99% of the total charge density is distributed within and above the first two atomic layers (represented by the solid circles in between the dashed lines) and peaks at the vacuum above the surface. They become typical surface resonances very quickly along $\bar{\Gamma}$-$\bar{X}$ as shown in Fig. 12(b). We can see from Figs. 12(c)–12(g) that there are many subsurface states (resonances) whose charge density distributes mainly under the surface. The $T5$ state at 0.4 $\bar{X}\bar{M}$ shows the characteristics of a subsurface state as discussed in Sec. IV B. It agrees with the theoretical finding shown in Fig. 12(d) where the charge profile peaks in the second atomic layer. Photoelectron cross section of the $T7$ state at $\bar{\Gamma}$ has been studied by the angle-resolved photoemission experiment as a function of photon energy in Ref. 17. It showed a bulk enhancement around $h\nu=21.0$ eV and a rather small peak around $h\nu=15.0$ eV. This state was called a subsurface state or resonance. The charge-density distribution from the calculation [Fig. 12(f)] agrees well with this previous experimental conclusion. More evidence has been found in this study. The $T9$ state at $\bar{M}$ is a subsurface resonance with the charge density residing in between the first and the second atomic layers as shown in Fig. 12(g). Its photoelectron cross section displays a relatively large enhancement near the bulk plasma frequency of Nb, as shown in Fig. 3.

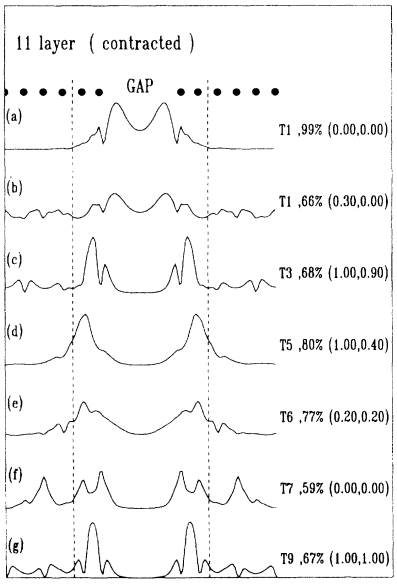

FIG. 12. Charge-density profiles $\rho(z)=\int\int dx\,dy\,\rho(\mathbf{r})$ of selected surface states (or resonances) at different $K_{\parallel}$. The positions of the atoms in the z direction are indicated by the dots. TN labels the Nth surface band (as discussed in the text), and the accompanying percentage value indicates the percentage of the integrated charge that resides on the top two layers of the slab (as marked by a dashed line). The position of each $K_{\parallel}$ in the surface Brillouin zone is indicated in the bracket.

E. Surface-layer contraction

It is very common for the outermost atomic layer of clean metal surfaces to show an inward relaxation (contraction). Charge redistribution often occurs among the first several layers. Large surface contraction affects the energy position and even the existence of surface energy bands, as found in the photoemission studies of Ta(001).[11] We found that when the surface is fully relaxed, the 12% inward relaxation of the top layer brings the calculated surface band structure into a better agreement with the

experimental results. The magnitude of the calculated relaxation also agrees well with the (13±5)% value determined from our photoelectron diffraction experiment.[22] Comparing the Nb(001) surface bands for an ideal surface (Fig. 1) and those for a relaxed surface (Fig. 2), and with the experiment, the most noticeable differences appear in the region along $\bar{\Gamma}$-$\bar{M}$ and $\bar{X}$-$\bar{M}$. When the 12% surface contraction is taken into consideration, the surface resonances ($S9$ and $S8$), which are not identified on an ideal surface, can be observed and the resonance $S3$ becomes more extended in the SBZ. It also shifts some surface bands to higher binding energies (e.g., $S6$) and some to lower binding energies (e.g., $S3$).

Surface contraction effects on the charge-density distribution at the Nb(001) surface have been analyzed in detail and can be summarized as follows: (1) The electron charge density located above the surface atoms and in the hollow region of the first atomic layer decreases. (2) The electron charge density existing between the first and the second atomic layers, mainly d electrons, is enhanced (especially for those near the center of the first interlayer). It shows that the d bonds in this region play a role in an inward relaxation of the surface layer. (3) The electron charge density in the hollow region of the second atomic layer decreases. It shifts to deeper layers.

V. CONCLUSION

We have performed systematic studies of the electronic structure of Nb(001) with angle-resolved photoemission experiments and self-consistent pseudopotential calculations. Ten surface bands have been identified experimentally throughout the SBZ. The self-consistent pseudopotential calculations found the existence of nine surface bands. The agreement for the initial-state properties and dispersion between experiment and theory is better for calculations of the 11-layer Nb(001) slab, which has been relaxed (with a 12% contraction of the first interlayer spacing). The surface resonance $S0$, which is not found in these nonrelativistic surface band calculations with either ideal or 12% contracted surfaces, is near E_F, and in the vicinity of pseudogap opened by the spin-orbit interaction.

Among these ten surface bands, three of them ($S2$, $S3$, and $S5$) are true surface states in absolute gaps, and six of them ($S1$, $S3$, $S4$, $S7$, $S8$, and $S9$) are surface resonances. $S6$ and $S0$ are surface states that exist in symmetry gaps. The surface contraction does not affect the energy position and dispersion of surface bands significantly except for those along $\bar{\Gamma}$-$\bar{M}$ and part of $\bar{X}$-$\bar{M}$. However, new surface resonances ($S9$ and $S8$) have been created and the $S3$ band has been extended to $\bar{M}$. Charge-density calculation shows an enhancement of charge density between the top two atomic layers and a small reduction at the first or the second atomic layers due to the contraction of the 11-layer Nb(001) slab surface.

ACKNOWLEDGMENTS

We greatly appreciate Professor R. H. Chen and Mr. J. C. Jan for the help of sample preparation. This work was supported by the SRRC and by the National Science Council, including a grant of computer time at the National Center for High-Performance Computing, under Grant No. (NSC)82-0208-M007-064 and Grant No. (NSC)83-0208-M194-014, Taiwan, Republic of China. Ames Laboratory is operated by Iowa State University for the U.S. Department of Energy under Contract No. W-F405-ENG-82 and is supported by the Director of Energy Research, Division of Material Sciences, including a grant of supercomputer time at NERSC. One of us (C.T.C.) thanks the Physics Department of National Chung-Cheng University for its hospitality.

[1]D. A. Papaconstantopoulos, *Hand Book of the Band Structure of Elemental Solids* (Plenum, New York, 1986).
[2]A. Zunger, G. P. Kerker, and M. L. Cohen, Phys. Rev. B **20**, 581 (1979).
[3]C.-L. Fu and K. M. Ho, Phys. Rev. B **28**, 5480 (1983).
[4]K. M. Ho, S. G. Louie, J. R. Chelikowsky, and M. L. Cohen, Phys. Rev. B **15**, 1755 (1977).
[5]R. H. Gaylord and S. D. Kevan, Phys. Rev. B **36**, 9337 (1987).
[6]P. L. Wincoff, N. B. Brookes, D. S. Law, and G. Thornton, Phys. Rev. B **33**, 4373 (1986).
[7]G. Jezequel, Y. Petroff, R. Pinchaux, and F. Yndurain, Phys. Rev. B **33**, 4352 (1986).
[8]B.-S. Fang, W.-S. Lo, and H.-H. Chen, Phys. Rev. B **47**, 10 671 (1993).
[9]G. S. Elliott, K. E. Smith, and S. D. Kevan, Phys. Rev. B **44**, 10 826 (1991).
[10]K. Jeong, R. H. Gaylord, and S. D. Kevan, Phys. Rev. B **38**, 10 302 (1988).
[11]X. Pan, E. W. Plummer, and W. Weinert, Phys. Rev. B **42**, 5025 (1990).
[12]R. Smoluchowski, Phys. Rev. **60**, 661 (1941).
[13]M. W. Finnis and V. Heine, J. Phys. F **4**, L37 (1974).
[14]C.-L. Fu, S. Ohnishi, E. Wimmer, and A. J. Freeman, Phys. Rev. Lett. **53**, 675 (1984).
[15]V. Heine and L. D. Marks, Surf. Sci. **165**, 65 (1986).
[16]M. Posternak, H. Krakauer, and A. J. Freeman, Phys. Rev. B **25**, 755 (1982).
[17]B.-S. Fang, C. A. Ballentine, and J. L. Erskine, Phys. Rev. B **38**, 4299 (1988).
[18]D. Shore and D. A. Papaconstantopoulos, Phys. Rev. B **35**, 1122 (1987).
[19]S. G. Louie, K.-M. Ho, and M. L. Cohen, Phys. Rev. B **19**, 1774 (1979).
[20]J. R. Anderson, D. A. Papaconstantopoulos, J. W. McCaffray, and J. E. Schirber, Phys. Rev. B **7**, 5115 (1973).
[21]S. G. Louie, K.-M. Ho, J. R. Chelikowsky, and M. L. Cohen, Phys. Rev. B **15**, 5627 (1977).
[22]W.-S. Lo, T.-S. Chien, B.-S. Fang, C. M. Wei, and W. N. Mei (unpublished).
[23]*Theory of the Inhomogeneous Electron Gas,* edited by N. H. March and S. Lundqvist (Plenum, New York, 1983), and references therein.
[24]N. Takeuchi, C. T. Chan, and K. M. Ho, Phys. Rev. Lett. **63**, 1273 (1989); C. T. Chan, K. P. Bohen, and K. M. Ho, *ibid.* **69**, 1672 (1992).
[25]K. M. Ho, C. Elsässer, C. T. Chan, and M. Fähnle, J. Phys. Condens. Matter **4**, 5189 (1992).
[26]E. Kneedler, K. E. Smith, D. Skelton, and S. D. Kevan, Phys. Rev. B **44**, 8233 (1991).